Metallic oxide p - I - n junctions with ferroelectric as the barrier

J. Yuan, H. Wu, L. X. Cao, L. Zhao, K. Jin, B. Y. Zhu, S. J. Zhu, J. P. Zhong, J. Miao, B. Xu, X. Y. Qi, X. G. Qiu, X. F. Duan, and B. R. Zhao

---

Articles you may be interested in

Optimal dielectric thickness for ferroelectric tunnel junctions with a composite barrier
J. Appl. Phys. **111**, 074311 (2012); 10.1063/1.3700245

Rectifying characteristic of perovskite oxide La 1 . 89 Ce 0 . 11 CuO 4 / Ba 0 . 5 Sr 0 . 5 TiO 3 / La 0 . 67 Sr 0 . 33 MnO 3 heterostructures
J. Appl. Phys. **110**, 103716 (2011); 10.1063/1.3662909

Preparation and dielectric characterization of ferroelectric (Pb x Sr 1 − x) Ti O 3 glass ceramics doped with La 2 O 3
Appl. Phys. Lett. **89**, 112908 (2006); 10.1063/1.2346136

Room temperature rectifying characteristics of epitaxial Y 1 Ba 2 Cu 3 − x Zn x O 7 − δ (x = 0.0 , 0.2) and Nb : Sr Ti O 3 (Nb: 0.05%, 0.1%, 0.5%) heterojunctions
J. Appl. Phys. **99**, 043906 (2006); 10.1063/1.2172867

Ferroelectric properties of laser-ablated Sr 1−x A x Bi 2 Ta 2 O 9 thin films (where A = Ba , Ca)
Appl. Phys. Lett. **80**, 637 (2002); 10.1063/1.1436528

Metallic oxide *p-I-n* junctions with ferroelectric as the barrier

J. Yuan, H. Wu, L. X. Cao, L. Zhao, K. Jin, B. Y. Zhu, S. J. Zhu, J. P. Zhong, J. Miao, B. Xu, X. Y. Qi, X. G. Qiu, X. F. Duan, and B. R. Zhao[a)]
National Laboratory for Superconductivity, Institute of Physics, Chinese Academy of Sciences, Beijing 100080, China and Beijing National Laboratory for Condensed Matter Physics, Chinese Academy of Sciences, Beijing 100080, China

The authors report the formation of the metallic oxide *p-I-n* junctions with the ferroelectric $(Ba, Sr)TiO_3$ (BST) as the barrier. The junctions with different thicknesses of BST are investigated. With appropriate thickness, the junctions possess definite parameters, such as the negligible reversed current density ($\leqslant 10^{-7}$ A/cm^2), large breakdown voltage (>7 V), and ultrahigh rectification ($>2 \times 10^4$) in the bias voltage $\leqslant 2.0$ V and temperature range from 5 to 300 K. It is under consideration that the built-in field V_0, the ferroelectric reversed polarized field V_{rp}, and the resistivity of the BST layer together decide the transport properties of the junctions. © *2007 American Institute of Physics*. [DOI: 10.1063/1.2711414]

In the past years, the oxide *p-n* (*p-I-n*) junctions has become an interesting topic for the purpose of developing the oxide electronics, and several types of junctions were created. One route is where a hole-doped oxide is deposited on the *n*-type semiconductor oxide to form the *p-n* junctions.[1–6] The other route is where the oxide insulator is used to sandwich the semiconductor *p*-type oxide and semiconductor *n*-type oxide to prepare the *p-I-n* junctions.[7–10] To develop the oxide electronics based on the functional oxides, such as optimally doped oxide superconductors and manganite, the *p-n* junctions which are made from optimally doped oxides are necessary. It is known that the origin of the rectifying function of the conventional semiconductor *p-n* junctions is the formed potential field, called the built-in field V_0 in the interface of the junction based on the energy band structure of *p*- and *n*-type semiconductors.[11] For the metallic *p*- and *n*-type oxides, the direct connection does not provide adequate barrier layer[12] and no rectifying function can be induced. Therefore introducing an appropriate barrier in the interface of the metallic *p-n* junction, i.e., making it into the metallic *p-I-n* junction, is a crucial topic. In the previous works, some insulator such as $SrTiO_3$ is used.[7–10] In order to make metallic oxide *p-I-n* junctions with strong functions, the perovskite structural ferroelectric was also used as the barrier,[13,14] since in the case of zero applied voltage, the ferroelectric can act as a usual insulator, in which a built-in field V_0 can form as in the conventional *p-I-n* junctions; under the external bias voltage, the ferroelectric possesses reversible polarization, resulting in the formation of a reversed polarized field V_{rp} in the junction.[15] Then, in contrast to the conventional insulator barrier, the ferroelectric barrier produces double potential fields, V_0 and V_{rp}, which may induce the rectifying function for the metallic oxide *p-I-n* junctions. The present work is focused on the preparation and understanding of *p-I-n* junctions with metallic oxide electrodes and ferroelectric barrier layer of different thicknesses.

In the present work, we developed a kind of metallic *p-I-n* junctions by using the ferroelectric $(Ba_{0.7}Sr_{0.3})TiO_3$ (BST) as the barrier layer, the metallic phase ferromagnetic

Sr-doped $LaMnO_3$, $(La_{0.67}Sr_{0.33})MnO_3$ (LSMO), with Curie temperature of ~ 350 K as the *p* region, and the optimally Ce-doped La_2CuO_4, T'-phase $(La_{1.89}Ce_{0.11})CuO_4$ (LCCO), with T_C of 30 K (the highest superconducting transition temperature in the electron-doped cuprate superconductor family[16,17]) as the *n* region. The junctions possess the definite negligible reversed current, large reversed voltage, and ultrahigh rectification in the low bias voltage ($\leqslant 2.0$ V) and in the temperature range of 5–300 K.

The *p-I-n* junctions of LCCO/BST/LSMO are prepared *in situ* by pulsed laser deposition method on (001) $SrTiO_3$ substrate; the growth conditions of BST and LSMO films were mentioned in previous works.[18,19] The thickness of each layer is controlled by the number of the pulses of the laser beam. Both LSMO and LCCO with thickness of ~ 100 nm and BST with thicknesses of 5, 15, 25, 50, and 100 nm are designed. All the junctions are in perfect epitaxial growth along the (001) direction. In Fig. 1, we present the high resolution tunneling electron microscopy (TEM) image of the cross section, the hysteresis loop of BST ~ 25 nm.

The transport properties of the junctions are influenced by the thickness of the BST layer. Figures 2(a)–2(e) show the *I-V* curves of the LCCO/BST/LSMO junctions with various thicknesses of BST at 5 K. The *I-V* characteristic reflects the evolution of the transport behaviors with increasing the thickness of BST. In the case of BST of ~ 5 nm, a standard single particle superconducting tunneling appears. The superconducting energy gap is obtained by being normalized with the background conductance, $G(V) = dI/dV \propto (d/dV)\int N_{FM}(\epsilon) N_{SC}(\epsilon+eV)[f(\epsilon)-f(\epsilon+eV)]d\epsilon$, with $N_{FM}(\epsilon) = N_{FM}(0)[1 + (|\epsilon|/\Delta)^\alpha]$, with $\alpha \simeq 0.8$, as shown in the inset of Fig. 2(a). When the thickness of BST is increased to 100 nm, the junction show a normal leakage current behavior through BST. In the low bias voltage, the current obeys Schottky model [inset of Fig. 2(e)], and obeys space-charge-limited model ($I \propto V^2$) in the high bias voltage. The resistivity of the junctions is mainly made up of two parts: $\rho_{jun} = \rho_{bar} + \rho_{BST}$; ρ_{bar} comes from the barrier which forms in the junction. The barrier shows different responses when bias of different directions is applied, which will be discussed below. ρ_{BST} is the intrinsic property of BST, which does not show asymmetry. The typical *p-n* junctions are obtained when

---

a)Electronic mail: yuanjie@ssc.iphy.ac.cn
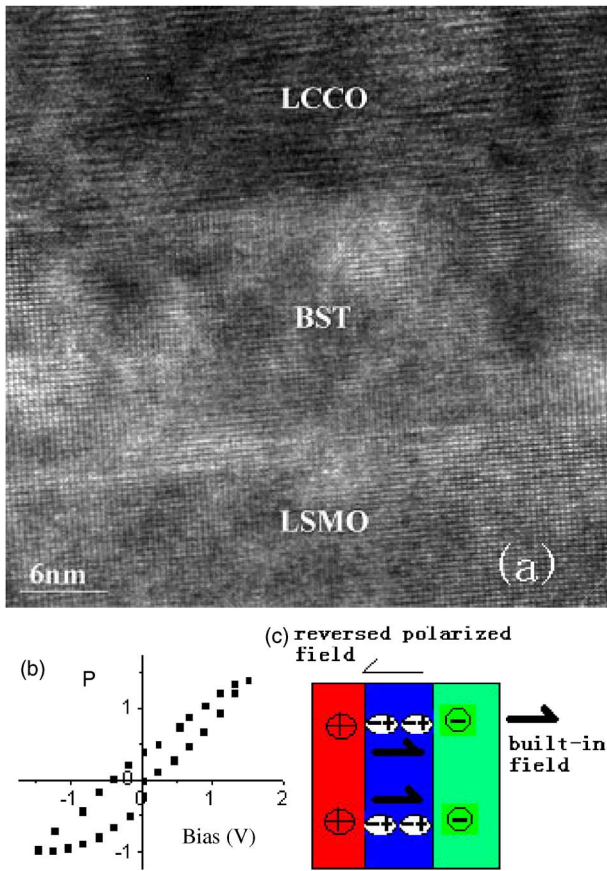
FIG. 1. (Color online) (a)High resolution TEM image of the cross section of the junction shows the perfect epitaxial growth of (001)LSMO/(001)BST/(001)LCCO on (001) SrTiO$_3$ substrate. (b) The hysteresis loop of BST layer of ~25 nm in the junctions. From (c) within the BST, the whole potential field is the series of V_{rp} and V_0 in several zones; the $V_{rp}+V_0$ blocks the reversed current.
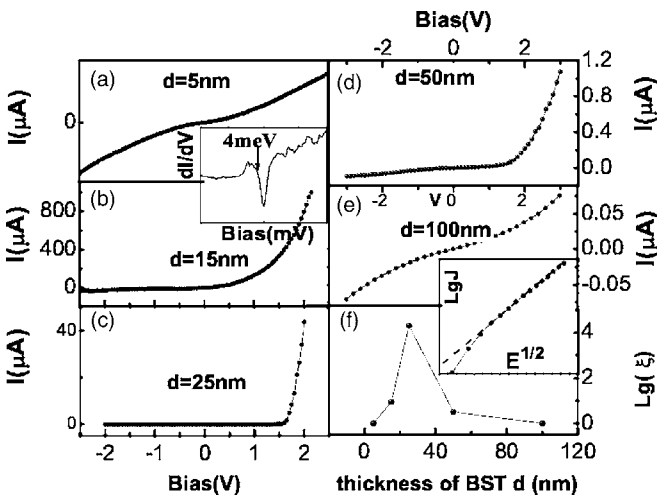
FIG. 2. *I-V* curves of the junctions with various thicknesses of BST at 5 K. (a) The thickness of BST is ~5 nm; the junction works as the conventional single particle superconducting tunneling junction, and it gives an energy gap of 4.0 meV for the LCCO [inset of (a)]. [(b)–(d)] With increasing the thickness, the *p-I-n* junction forms and the asymmetry enhances; the largest rectification (>10^4) is obtained for BST of ~25 nm (c). (e) The BST is as thick as 100 nm, and it acts as a block ferroelectric layer to limit the leakage current between *p* and *n* regions; the current shows Schottky model in the low electric field (see the inset) and space-charge-limited model in the high electric field (not shown in the figure). (f) The role of the thickness of BST layer on rectifying function in the present junction.
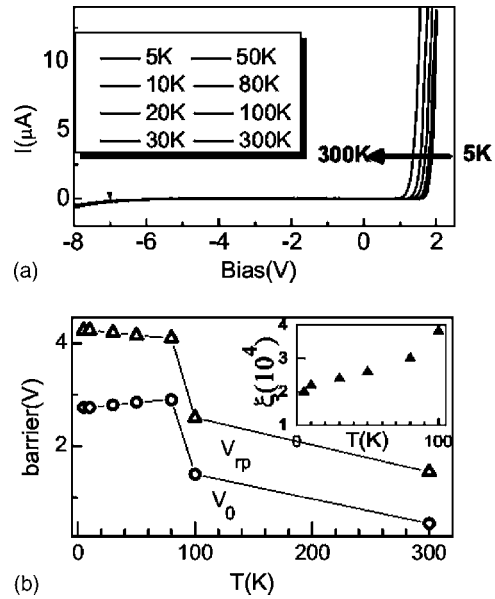
FIG. 3. (a) *I-V* curves at various temperatures for the LCCO/BST/LSMO *p-I-n* junction with BST of ~25 nm. It basically shows the temperature independence of the shape of the *I-V* curves. (b) The V_0 and V_{rp} are estimated from (a). The V_{rp}/V_0 increases with increasing temperature; this indicates the positive temperature dependence of rectification of the *p-I-n* junction (shown in the inset).

BST is 20–25 nm thick; in this thickness range of BST, ρ_{bar} determines the rectifying function, and the largest rectification is ≥2×10^4 [Fig. 2(f)]. When the BST layer gets thicker, ρ_{BST} increases and dominates ρ_{jun} step by step. The junction shows the behavior like BST.[20]

In order to reveal the ferroelectric role on the LCCO/BST/LSMO junction further, we investigated the temperature dependence of the rectifying function of the junction with BST of ~25 nm. Figure 3(a) shows *I-V* curve shape of the LCCO/BST/LSMO junction with BST of ~25 nm in the temperature range from 5 to 300 K. But the temperature dependence of rectification is needed to be understood; to define this, we search the relation of the rectification and $V_0(V_{rp})$. We characterize V_0 and V_{rp} in the following two critical points: the forward bias (potential height of the junction) at which the forward current starts to occur is the value of $V_{rp}-V_0$, and the reversed bias (the breakdown field of the junction) at which the reversed current starts to occur (the criterion is 1×10^{-5} A/cm^2 at 5 K) is the value of the sum of $V_{rp}+V_0$. For the junction with BST of ~25 nm, at 5 K, the forward current starts to occur at 1.5 V, and the reversed current starts to occur at −7 V, and then V_{rp}=4.25 V and V_0=2.75 V. By this way, every couple of V_0 and V_{rp} at each temperature can be defined and concluded in Fig. 3(b). At 5 K, the rectification, defined as ξ=forward current at +2 V/reversed current at −2 V, is 2.2×10^4. When the temperature is increased from 10 to 80 K, the rectification changes from 2.3×10^4 to 3×10^4 and up to 3.8×10^4 at 100 K. So the rectification of the present *p-I-n* junctions shows obvious positive temperature dependence in the temperature range [the inset of Fig. 3(b)]. The big change of V_{rp} and V_0 of the junction at ~100 K may come from a phase transition of BST in the junction with such nanometer size. This should be examined further. This big change looks to lead the large increase of the rectification at 100 K. The above fact clearly indicates that with increasing temperature,

the V_0 and V_{rp} decrease, but the V_{rp} becomes more strong or to dominate the rectification than the V_0 does when the temperature is increased (V_{rp}/V_0 increases with increasing T). It should be noted that for this kind of *p-I-n* junctions, the bias voltage is $1-2$ V, which is much larger than the superconducting energy gap of LCCO, so these junctions all work on the normal state transport in metallic state of LCCO. The LSMO is also in metallic state in the temperature range of $5-300$ K. So both LCCO and LSMO should not have the role of enhancing the forward current and rectification from 5 to 300 K. Therefore the above positive temperature coefficient of rectification must come from V_0 and V_{rp} in BST; the LCCO and LSMO just provide the electron and hole carriers.

In conclusion the metallic oxide LCCO/BST/LSMO *p-I-n* junctions consisting of three main kinds of functional oxides are fabricated. The optimally electron doped high-T_C superconductor LCCO is used as the *n* electrode. With different thicknesses of BST layer, the junctions show different transport behaviors. In an appropriate range, the ferroelectric barrier leads double potential fields V_0 and V_{rp} to dominate the rectification of the junction, for which the positive temperature coefficients are clearly obtained, and make the junction to be real potential basic devices in the field of oxide electronics.

[1] H. Tanaka, J. Zhang, and T. Kawai, Phys. Rev. Lett. **88**, 027204 (2002).
[2] A. Tiwari, C. Jin, D. Kumar, and J. Narayan, Appl. Phys. Lett. **83**, 1773 (2003).
[3] F. Hu, J. Gao, J. R. Sun, and B. G. Shen, Appl. Phys. Lett. **83**, 1869 (2003).
[4] H. B. Lu, S. Y. Dai, Z. H. Chen, Y. L. Zhou, B. L. Cheng, K. J. Jin, L. F. Liu, G. Z. Yang, and X. L. Ma, Appl. Phys. Lett. **86**, 032502 (2005).
[5] X. X. Xi, C. Doughty, A. Walkenhorst, S. N. Mao, Qi Li, and T. Venkatesan, Appl. Phys. Lett. **61**, 2353 (1992).
[6] W. Ramadan, S. B. Ogale, S. Dhar, L. F. Fu, N. D. Browning, and T. Venkatesan, J. Appl. Phys. **99**, 043906 (2006).
[7] M. Sugiura, K. Uragou, M. Noda, M. Tachiki, and T. Kobayashi, J. Appl. Phys. **90**, 187 (2001).
[8] C. Mitra, P. Raychaudhuri, G. Köbernik, K. Dörr, K.-H. Mller, L. Schultz, and R. Pinto, Appl. Phys. Lett. **79**, 2408 (2001).
[9] P. L. Lang, Y. G. Zhao, B. Yang, and X. L. Zhang, Appl. Phys. Lett. **87**, 053502 (2005).
[10] Yu. A. Boikov, E. Olsson, and T. Claeson, Phys. Rev. B **74**, 024114 (2006).
[11] B. G. Streetman, *Solid State Electronic Devices*, 2nd ed. (Prentice-Hall, Englewood Cliffs, NJ, 1980), p. 148.
[12] J. Mannhart, A. Kleinsasser, J. Strobel, and A. Baratoff, Physica C **216**, 401 (1993).
[13] Y. Watanabe, Phys. Rev. B **57**, R5563 (1998).
[14] I. Grekhov, L. Delimova, I. Liniichuk, D. Mashovets, and I. Veselovsky, Physica E (Amsterdam) **17**, 640 (2003).
[15] Y. E. Tsymbal and H. Kohlstedt, Science **313**, 181 (2006).
[16] M. Naito and M. Hepp, Jpn. J. Appl. Phys., Part 2 **39**, L485 (2000).
[17] L. Zhao, H. Wu, J. Miao, H. Yang, F. C. Zhang, X. G. Qiu, and B. R. Zhao, Supercond. Sci. Technol. **17**, 1361 (2004).
[18] B. Chen, H. Yang, L. Zhao, J. Miao, B. Xu, X. G. Qiu, B. R. Zhao, X. Y. Qi, and X. F. Duan, Appl. Phys. Lett. **84**, 583 (2004).
[19] F. C. Zhang, W. Z. Gong, C. Cai, B. Xu, X. G. Qiu, R. Vanfleet, L. Chow, and B. R. Zhao, Solid State Commun. **131**, 271 (2004).
[20] H. Yang, K. Tao, B. Chen, X. G. Qiu, B. Xu, and B. R. Zhao, Appl. Phys. Lett. **83**, 1611 (2003).